SERRATED YIELDING IN A NICKEL-BASE SUPERALLOY

Eric S. Huron

Engineered Materials Technology Laboratories
GE Aircraft Engines
Cincinnati, OH 45215

Abstract

Serrated yielding, also called discontinuous yielding or jerky flow, occurs in many metals when deformed at particular combinations of strain rate and temperature. It has been observed in superalloys such as IN600, IN718 or Waspaloy at temperatures in the range of 400C. In this investigation serrated yielding was examined in the superalloy Rene'88DT. Serrated yielding was of interest in this alloy because it interfered with reliable tensile testing and caused strain overshoots and load shifts in strain-controlled Low Cycle Fatigue (LCF) testing. The objectives of the test program were to eliminate the testing problems, determine the metallurgical mechanism, and assess impact on component performance.

Tensile tests were conducted at both constant strain rate and constant crosshead speed at various combinations of strain rate and temperature. The character and degree of the observed serrations were influenced by the control mode. Some tests were interrupted at intermediate strain levels to study the dislocation substructure associated with serrated yielding. Serrated yielding was not observed in tests performed at 204C or 649C. It was observed at all strain rates tested at 399C, but only above 0.0005/sec at 454C and 593C, and only above 0.00008/sec at 538C. The strain to reach the first serration increased with increasing temperature for a given strain rate. For a given temperature, the strain to reach the first serration increased with decreasing strain rate. The mechanism was concluded to be interaction of carbon or other solute atoms with dislocations, essentially a form of dynamic strain aging. The activation energy for this mechanism in Rene'88DT was calculated to be 0.72 eV, or 16,560 cal/mole, a value which agreed well with literature data.

The results of the tensile study were used to develop a modified LCF test procedure. This consisted of using strain control at a reduced frequency in the first portion of the test, were serrations were most likely to occur, followed by completing the test in a normal manner at typical test frequencies. This procedure significantly reduced the number of problem tests due to missed target strain levels. For actual components, serrated yielding was assessed to have no impact because highly stressed areas of parts subjected to LCF are typically constrained by surrounding material and are unlikely to experience instantaneous displacements.

Superalloys 1992
Edited by S.D. Antolovich, R.W. Stusrud, R.A. MacKay,
D.L. Anton, T. Khan, R.D. Kissinger, D.L. Klarstrom
The Minerals, Metals & Materials Society, 1992

Introduction

Serrated yielding is common in many metals. Examples include the classic upper and lower yield point caused by static strain aging in low carbon steels (1) and the dynamic strain aging observed in aluminum (2,3). These effects are generally explained by interstitial atoms pinning dislocations. Dynamic strain aging occurs when the strain rate is at some intermediate value that allows interstitial atoms to diffuse to the dislocation cores quickly enough to re-pin the dislocations after initial yielding. This is observed as repeated serrations throughout the stress strain curve. This mechanism is also believed to operate in Ni-base alloys (4-7).

Several general patterns are typical of dynamic strain aging. If the strain rate is plotted on log scale against 1/T, serrated yielding tends to occur in an intermediate temperature range (4-7). This indicates that serrated yielding is a thermally activated process and therefore it can be explained by an equation of the form:

$$\dot{\epsilon}_c = A\mu^{-b} \epsilon_c^{n} \exp(-H/kT)$$

where $\dot{\epsilon}_c$ is the critical strain rate, μ is the grain size, ϵ_c is the critical strain at which serrations occur, and H is the activation energy associated with the process. A, b, and n are material constants. According to this equation, for constant grain size, the slope of the log ϵ_c vs. 1/T plot at constant strain rate is H/nk. The slope of a plot of $\log \dot{\epsilon}_c$ vs. $\log \epsilon_c$ at constant temperature is n.

The mechanism claimed to explain this behavior is solute atom core drag of dislocations, where interstitial atoms locate preferentially in the expanded lattice at the core of a dislocation, and once so located pin the dislocations. The activation energy for dislocation core interstitial diffusion is typically 0.2-0.5 eV for most metals and is usually about half the activation energy for matrix interstitial diffusion (8). The activation energy reported for Ni-C alloys (4) of 0.63 eV is slightly less than half the activation energy for matrix diffusion of carbon in nickel, which is 1.5 eV (7).

Serrated yielding has been observed in the Ni-base superalloy Rene'88DT. The goal of this study was to determine the mechanism for this behavior and determine ways to minimize its impact on LCF testing.

Procedure

Standard tensile specimens with 6.35 mm gage diameters and Low Cycle Fatigue (LCF) specimens with uniform 10.2 mm gage diameters were used for this program. The material was taken from a R'88DT F110 Low Pressure Turbine Disk. The composition of R'88DT is given in Table 1. The alloy

Table 1: Composition of Rene'88DT (weight percent)

Co	Cr	Mo	W	Al	Ti	Nb	B	C	Zr	Ni	Predicted γ' volume fraction
13	16	4	4	2.1	3.7	0.7	0.015	0.03	0.03	bal	40

is processed using powder metallurgy techniques, by isothermal forging of extruded billet, followed by heat treatment to achieve an ASTM 7/8 grain structure. The processing of R'88DT is described in detail elsewhere in these proceedings (9).

Room and elevated temperature tensile tests were conducted over a range of strain rates from 0.00001/sec to 0.1/sec. Elevated temperatures were performed using a clamshell resistance furnace. Most tests were performed at constant strain rate, but two tests were performed at constant cross-head speed at 399C, using MTS servohydraulic test equipment. Some earlier data generated using an older rigid Baldwin tensile machine were included in the analysis. The Baldwin testing was done with a nominally constant strain rate of 0.00008/sec to yield, followed by an increased rate of 0.0008/sec to failure. Twenty-five tests were conducted to failure at room temperature, 204C, 399C, 538C, and 649C. An additional twenty-five interrupted tests were conducted at 399C, 454C, 538C, 593C, and 649C. After reaching 10% elongation, these tests were cycled immediately to zero load, using the MTS programmable controller.

Some of the interrupted test specimens were analyzed using optical metallography and Transmission Electron Microscopy. Standard specimen preparation techniques were used.

LCF tests to study the application of the tensile testing to improving LCF test control were performed using strain control mode and a variety of waveforms, described in the Results section. All testing was done using servohydraulic machines, induction heating for specimen temperature control, and standard extensometry.

Results

Results of Tensile Test Study

Mechanical property data are summarized in Table 2. For conditions with multiple tests, the data were averaged. Tracings of representative load-elongation curves are shown in Figure 1. No serrations were observed

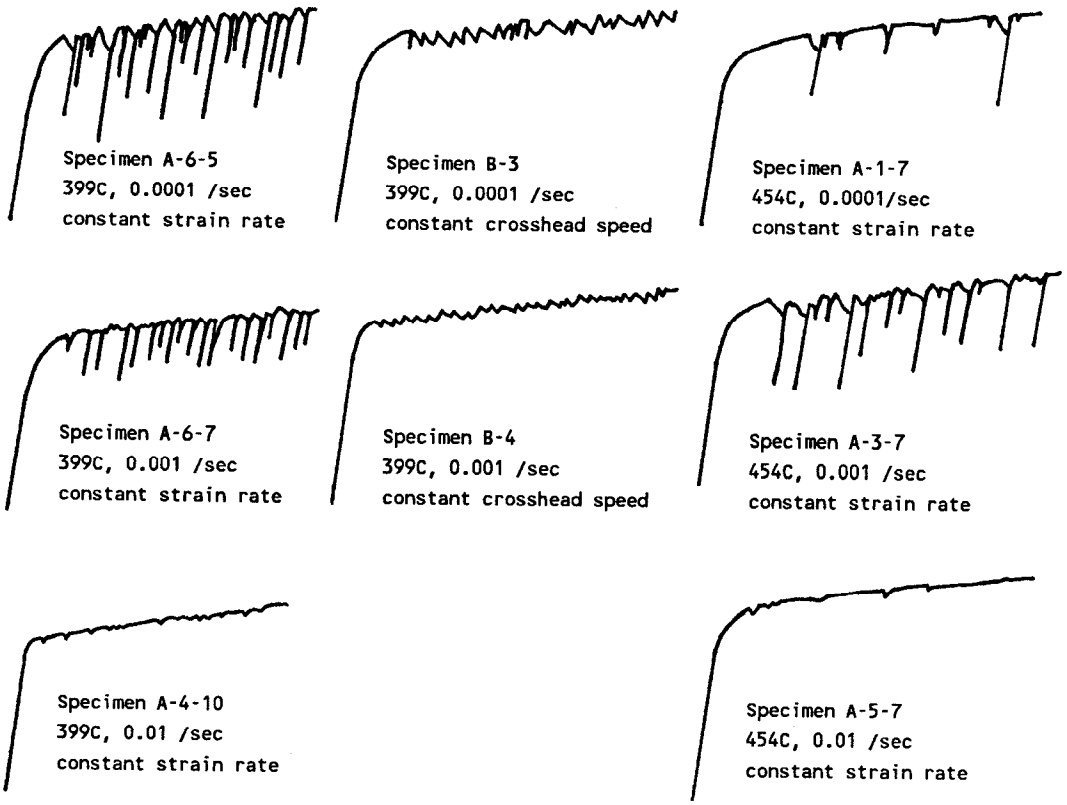

Figure 1: Schematics of Load-Elongation Curves for Representative Tests

Table II: Averaged Mechanical Property Data Used for Calculations

Temp. (C)	No. of Data Points	Strain Rate (/sec)	0.2% Yield Strength (MPa)	Ult. Tensile Strength (MPa)	Critical Strain to Serration	Reciprocal Temperature (deg. K)
25	1	.00001	1230.1	1605.8	none	.00337
25	1	.0001	1232.8	1614.1	none	.00337
25	1	.001	1243.2	1605.2	none	.00337
25	1	.01	1258.3	1616.9	none	.00337
25	1	.1	1279.7	1548.6	none	.00337
204	1	.00001	1122.5	1568.6	none	.00209
204	1	.0001	1125.9	1574.1	none	.00209
204	1	.001	1130.8	1570.7	none	.00209
204	1	.01	1131.5	1558.0	none	.00209
204	1	.1	1150.1	1563.1	none	.00209
399	1	.00001	1137.7	1548.6	.01560	.00149
399	19	.00008	1106.6	n/a	.01290	.00149
399	3	.0001	1089.4	1550.0	.01187	.00149
399	1	.0005	1093.5	interrupted	.01060	.00149
399	3	.001	1090.1	1550.0	.00853	.00149
399	1	.005	1021.1	interrupted	.00840	.00149
399	2	.01	1062.5	1452.1	.00780	.00149
399	1	.1	1081.8	1519.0	.00700	.00149
454	1	.0001	1113.5	interrupted	.02	.00137
454	1	.0005	1092.9	interrupted	.0136	.00137
454	1	.001	1088.7	interrupted	.0138	.00137
454	1	.005	1086.7	interrupted	.0108	.00137
454	1	.01	1069.7	interrupted	.0104	.00137
538	1	.00001	1094.2	1574.1	none	.00123
538	5	.00008	1051.5	n/a	.05500	.00123
538	2	.0001	1114.9	1558.3	.005	.00123
538	1	.0005	1131.5	interrupted	.03300	.00123
538	2	.001	1130.1	1491.4	.0200	.00123
538	1	.005	1121.1	interrupted	.03680	.00123
538	2	.01	1104.2	1427.3	.01210	.00123
538	1	.1	1081.8	1457.6	.01000	.00123
593	1	.00008	1270.7	n/a	.068	.00115
593	1	.0001	1115.6	interrupted	none	.00115
593	1	.001	1132.2	interrupted	none	.00115
593	1	.01	1112.2	interrupted	.024	.00115
649	1	.00001	1066.0	1250.8	none	.00108
649	2	.0001	1085.9	1376.2	none	.00108
649	1	.0005	1110.1	interrupted	none	.00108
649	2	.001	1084.6	1547.3	none	.00108
649	1	.005	1059.1	interrupted	none	.00108
649	2	.01	1069.1	1502.4	none	.00108
649	1	.1	1081.8	1445.9	none	.00108

at 25C, 204C, or 649C. At 399C, serrations were present at all strain rates, but were most distinct and produced the largest load drops at the slowest strain rates. Serrations were observed at all strain rates at 454C as well, but there were fewer serrations at the lowest strain rate than for 399C. At 538C, serrations were not observed at 0.00001/sec, and were observed in only one of two tests at 0.0001/sec, but were observed at all other strain rates. At 593C, for the tests performed on the MTS machine, serrations were only observed at the highest strain rate tested of

0.01/sec, but one bar from the earlier Baldwin tests showed serrations at 0.00008/sec. The temperature and strain rate regions where serrations were observed are mapped in Figure 2.

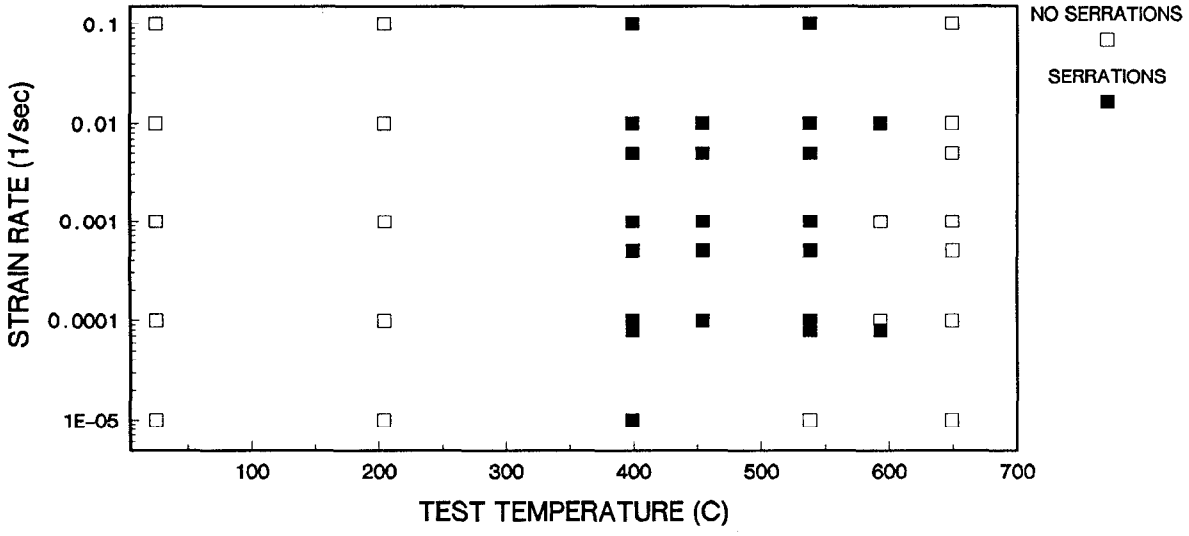

Figure 2: Serrated Yielding Occurrence by Strain Rate and Temperature

For similar nominal strain rates, tests done in strain control showed larger load drops than the stroke control tests. This is probably due to improved response of the testing machine in stroke control, allowing more rapid sensing of the serration and compensation by the machine.

The strain to first serration (ϵ_c) showed a strong correlation with strain rate for each temperature (Figure 3a). Two datapoints at 538C did not fit the rest of the data. The slopes were negative: at lower strain rates a larger strain occurs before serrated yielding begins. Note that the slope for each temperature changed, with decreasing slope with increasing temperature, so the combined temperature data showed reduced correlation (Figure 3b). As Figure 4a shows, ϵ_c also showed a correlation when plotted against 1/T for each strain rate. There was a trend of decreasing slope with increasing strain rate, but overall the slopes were similar. The slope of this curve has physical significance because it is proportional to the activation energy for the mechanism controlling serrated yielding. For this calculation the data for all strain rates were combined (Figure 4b).

The microstructures of selected bars tested to 10% strain representing extremes of serrated yielding behavior were examined optically and by TEM. The density of twins or slip lines within the grains was higher for deformed gage sections relative to undeformed threaded ends, but between bars that showed a high degree of serrated yielding and those that did not, there were no apparent differences (Figure 5). The TEM results also failed to show any pattern between specimens with different degrees of serrated yielding, or any clear evidence of mechanical twinning (Figure 6). All the specimens showed high concentrations of unit dislocations and stacking faults, indicating that the 10% strain level may have been too high for TEM observation. One specimen showed a slight tendency towards distinct slip bands. The dark field image of the 399C, 0.0001/sec specimen indicated light streaks that may have been microtwins, but these may also have been stacking faults, because the two features create similar contrast. The streaks were very thin.

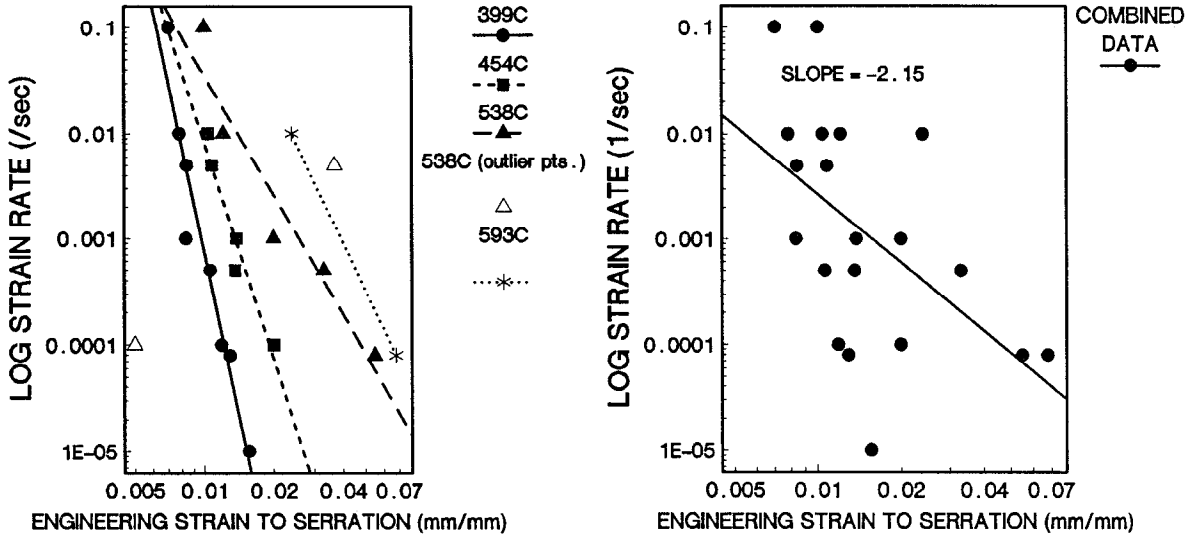

a) Individual Temperatures b) All Temperatures Combined

Figure 3: Strain Rate vs. Critical Strain to Reach First Serration

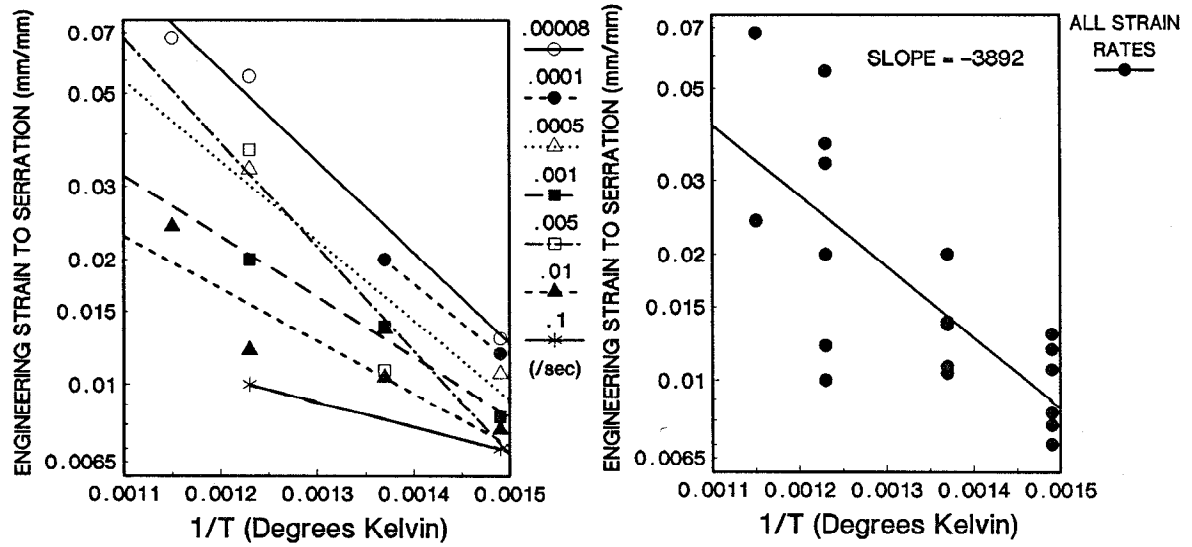

a) Individual Strain Rates b) All Strain Rates Combined

Figure 4: Critical Strain to Reach Serration vs. Temperature

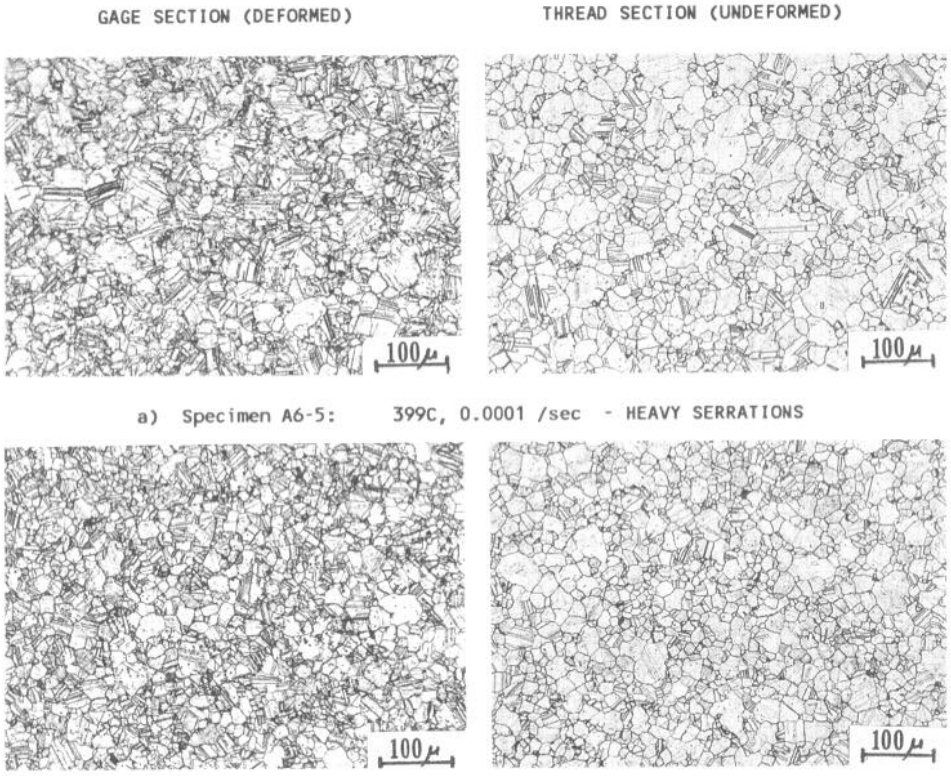

Figure 5: Optical Micrographs of Representative Specimens. The gage sections appear to have more twins or slip lines present than the thread sections. There is no correlation with degree of serrations.

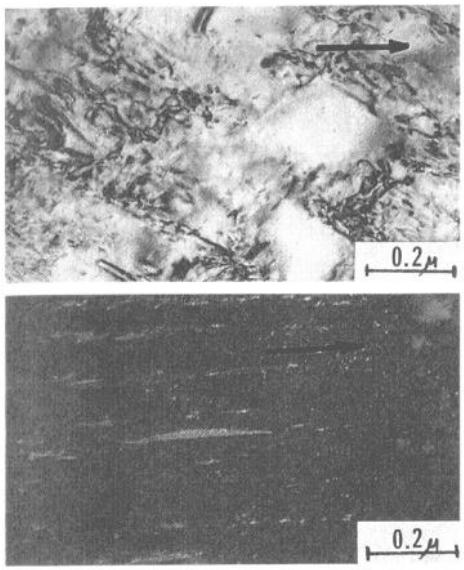

Specimen A6-5: 399C, 0.0001 /sec, heavy serrations. [001] bright field image in top photo; reflection from [110] possible microtwin or stacking fault for bottom photo.

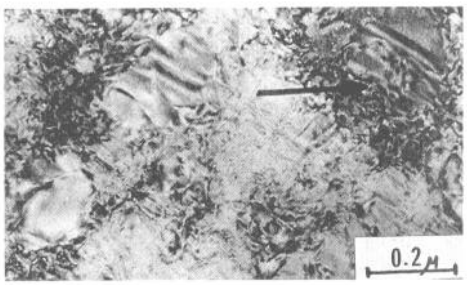

Specimen A2-10: 649C, 0.01 /sec, no serrations. [001] bright field image.

Figure 6: TEM Micrographs of Representative Specimens. Structures were similar regardless of degree of serrated yielding observed.

Results of LCF Test Study

In LCF testing, serrated yielding tends to either cause the test to jump beyond its assigned level in the early portion of the test when the strain range is being established, or causes a shift to a lower stress level and lower A-ratio once the strain range stabilizes during the mid-life of the test. A series of LCF tests at 399C were made at incrementally reduced strain rates until a strain rate was found where serrations stopped occurring. Three bars were run using standard conditions of 30 cpm, triangle wave, A = 1.0. The nominal strain rate was 0.007/sec, and all bars showed severe first cycle or early life serrations. Next, three bars were run at a reduced strain rate of 0.0016/sec. These bars showed moderate early-life serrated yield events. Three bars were then run at 0.0008/sec and showed no early-life serrations, but severe mid-life serrations. Finally, seven tests were run with a very low strain rate of 0.0004/sec. This strain rate was maintained only for 100 cycles, then was increased to 0.007/sec and the strain maximum was reduced by 0.02% (typically resulting in an alternating pseudostress reduction of 10 MPa). One bar in this group had a minor serrated yielding event.

The resulting recommended LCF test procedure consisted of a triangle wave at 0.025Hz at maximum strain for 100 cycles, then beginning cycle 101 at 0.5Hz, at maximum strain minus 0.02% (0.0002 mm/mm) without interruption, then continuing in strain control for 24 hours. After 24 hours a switch was made to load control at 5Hz to failure. The procedure required a specialized function generator to make smooth changes between waveforms. This procedure was successfully applied to a specific R88DT testing program. Approximately 80% of bars tested with the old procedure had first cycle serrations with strain overshoots as high as 30%, while over 300 bars were tested with the new procedure without any serrations.

Discussion

Serrated yielding has been studied in Ni-base alloys of varying complexity. Most metals show positive slopes for both the $\dot{\epsilon}_c$ vs. ϵ_c curve and the ϵ_c vs. 1/T curve. This was observed for simple Ni-C alloys (4) and IN600 (6), a solid solution strengthened alloy. Some constrasting behavior was noted for Waspaloy, an age-hardened alloy similar to Rene'88DT (6). At low temperatures solutioned and aged Waspaloy displayed a positive slope of the $\dot{\epsilon}_c$ vs. ϵ_c curve, and an activation energy of 0.58 eV. However, at 315C, Waspaloy showed a reversal in the slopes of the $\dot{\epsilon}_c$ vs. ϵ_c and ϵ_c vs. 1/T curves. The activation energy for the higher temperature deformation was 1.37 eV if calculated from the reversed ϵ_c vs. 1/T curves. An alternate method of calculating activation energy based on stress decrement, measured from the drops in the stress-strain curve, did not result in a reversal in slope and gave an activation energy of 0.68 eV over all temperatures.

Hayes and Hayes (6) proposed that the reversal in slope of the ϵ_c vs. 1/T curve indicated a delay on the flow curve to the start of serrated yielding, caused by the carbon atoms being tied up in some way other than the pinning of dislocations during early deformation. Solutioned and quenched Waspaloy (no aging) did not show the reversed ϵ_c behavior, and serrated behavior occurred early in the plastic region of the test. It was concluded that the γ' precipitate caused the delay by serving as a carbon sink. Serrated yielding did not occur until dislocations were arrested by the γ', and during the delay period from that arrest, carbon diffused from the γ' or the $\gamma - \gamma'$ interface to the dislocations. The authors proposed that the higher activation energy represented the formation of a

complex $Ni_3(Ti,Al,C)$ precipitate. Similarly, Blakemore (7) suggested that the occurrence of serrations in carburized nickel corresponded to the dissolution of Ni_3C carbides.

The R'88DT results were similar to those reported for Waspaloy in the high temperature regime. The slopes of the $\dot{\epsilon}_c$ vs. ϵ_c curve and the ϵ_c vs. 1/T curves were negative (Figures 3 and 4). There was evidence of an increasingly negative slope with decreasing temperature in Figure 3, but Rene'88DT did not show the inversion in the slope of the $\dot{\epsilon}_c$ vs. ϵ_c curve at low temperatures. Indeed, Rene'88DT did not show any serrated yielding below 399C. The slope of the $\dot{\epsilon}_c$ vs. ϵ_c curve is n. The reason for the changing slopes at different temperatures for Rene'88DT was not clear. The value of n for Waspaloy was essentially constant above 427C (6). No physical basis for n has been proposed, and n is usually treated as constant, so the Rene'88DT data at all temperatures was combined to give a value for n of -2.15. This compares to values of -2 for Waspaloy at high temperatures and 0.74 for IN-600 (6), and 0.63 for Ni-C alloys (4). The apparent activation energy for R'88DT was calculated as 0.72 eV, or 16,560 cal/mole. This agrees well with reported values of 0.63 eV for Ni-C (4), and 0.56-0.60 eV for IN-600 and 0.56-0.68 eV for Waspaloy (6), but is much higher than the value of 0.26 eV measured for carburized nickel (7).

The strain rate sensitivities were calculated using the 0.2% yield strength values. For room temperature and 204C the strain rate sensitivity was always positive, and was predominantly positive at 649C. For all other temperatures the strain rate sensitivity was predominately negative. This agreed with results for IN-600 (5,6) in that serrated yielding tended to occur in regions of negative strain rate sensitivity.

The present R'88DT results and calculated activation energy agree closely with the results for other Nickel alloys: Ni-C, IN600, and in particular Waspaloy. The same mechanism, interstitial atom interaction with dislocations, is believed to cause serrated yielding. This is supported by the lack of visible microstructural evidence of twinning or slip character changes between samples that showed serrated yielding and those that did not, and by the fact that serrated flow is generally not observed in pure Ni alloys in the absence of carbon (5). The critical strain has been correlated with carbon content (4). A study of the effect of different carbon contents in Rene'88DT would be of interest. Additionally, Rene'88DT with various heat treatments could be tested to study the role of γ' presence and morphology and grain size on serrated yielding.

The same mechanism is believed to operate in LCF testing. Twinning has been proposed as a mechanism for serrated yielding in LCF of IN718 (10,11), but no conclusive proof between samples showing serrated yielding and twinning has been shown. In LCF testing, serrated yielding has two negative practical impacts. The first impact is the nuisance of having tests not meet the goal strain level. More importantly, intuitively it would seem that tests which showed load drops from mid-life serrated yield events would have longer lives due to the lower maximum stresses, although available data failed to show this. For actual hardware serrated yielding was considered to have little impact, as regions of components typically subjected to LCF are usually constrained by much thicker unyielding sections in the adjacent areas of the part, so if a serrated yielding event occurs, there will be no instantaneous strain displacement. Based on this argument it appears the problem of serrated yielding is limited to a testing annoyance, but it represents an area of the mechanical behavior of superalloys which needs further understanding.

Conclusions

1. Serrated yielding in R'88DT was observed between the temperatures of 399C and 593C. Serrated yielding occurred at all strain rates at 399C, but was only observed at strain rates above 0.0005/sec at 454C and 593C, and only above 0.00008/sec at 538C.

2. The critical strain to reach the first serration (ϵ_c) increased with increasing temperature for a given strain rate. For a given temperature, ϵ_c increased with decreasing strain rate.

3. The probable mechanism for the serrated yielding is the interaction of carbon atoms with dislocations by dynamic strain aging. The activation energy for this interaction in R'88DT was determined to be 0.72 eV, or 16,560 cal/mole, which agreed closely with literature values.

4. A modified LCF procedure using slower strain rates for the first 100 cycles was successful in eliminating serrated yielding from the LCF tests.

Acknowledgements

The author thanks General Electric Aircraft Engines for permission to publish this work, Sue Renner for manuscript preparation, Dr. Paul Roth of GE for help with the LCF program, and Dr. Robert Field of GE for the TEM work. Bill Grieszmer and David Wingerberg of Metcut Research Associates, Cincinnati, OH, executed the specialized tests.

References

1. A. Van Den Beukel and U. F. Kocks, "The Strain Dependence of Static and Dynamic Strain-Aging," Acta Met., 30 (1982), 1027-1034.

2. P. G. McCormick, "The Portevin-LeChatelier Effect in An Al-Mg-Si Alloy," Acta Met., 19 (1971), 463-471.

3. E. Pink and A. Grinberg, "Stress Drops in Serrated Flow Curves of Al-5Mg,", Acta Met., 30 (1982), 2153-2160.

4. Y. Nakada and A. S. Keh, "Serrated Flow in Ni-C Alloys," Acta Met., 18 (1970), 437-443.

5. R. A. Mulford and U. F. Kocks, "New Observations on the Mechanisms of Dynamic Strain Aging and of Jerky Flow," Acta Met., 27 (1979), 1125-1134.

6. R. W. Hayes and W. C. Hayes, "On the Mechanism of Delayed Discontinuous Plastic Flow in an Age-Hardened Nickel Alloy," Acta Met., 30 (1982), 1295-1301.

7. J. S. Blakemore, "The Portevin-Le Chatelier Effect in Carburized Nickel Alloys," Met. Trans., 1 (1970), 1281-1285.

8. D. Hull and D. J. Bacon, Introduction to Dislocations, 3rd Ed., Pergamon Press, Oxford (1984), 225.

9. D. Krueger, R. D. Kissinger, and R. G. Menzies, "The Development and Introduction of a Damage Tolerant High Temperature Nickel-Base Disk Alloy, Rene'88DT," elsewhere in these Proceedings.

10. D. Fournier and A. Pineau, "Low Cycle Fatigue Behavior of Inconel 718 at 298K and 823K," Met. Trans., 8A (1977), 1095-1105.

11. T. H. Sanders Jr., R. E. Frishmuth, and G. T. Embley, "Temperature Dependent Deformation Mechanisms of Alloy 718 in Low Cycle Fatigue," Met. Trans., 12A (1981), 1003-1010.